Supporting Information

Phillips *et al.* 10.1073/pnas.0801988105

SI Methods

Cell Culture and Reagents. Primary fibroblasts were harvested from 8- to 16-week-old male Wistar rats by enzymatic digestion of the dermal skin layer (1). Cells were expanded in growth media consisting of DMEM, 10% fetal bovine serum (FBS), and 1% penicillin-streptomycin. Antibiotics and cell culture media were obtained from Invitrogen (Carlsbad, CA). FBS was purchased from HyClone (Logan, UT), and all other cell culture supplements and reagents were acquired from Sigma (St. Louis, MO).

Retrovirus Production. The pTJ66-Runx2 retroviral vector utilizes the promoter activity of a 5′ long terminal repeat to express a single, bicistronic mRNA encoding the murine cDNA for the type II MASNSLF Runx2 isoform followed by an internal ribosomal entry site and a Zeocin resistance-enhanced green fluorescent fusion protein (2, 3). Empty vector control plasmid lacked the Runx2 insert. The MLV-Gag-RFP retroviral vector enables visualization of red fluorescent protein (RFP)-labeled retrovirus by expressing a gag-RFP fusion protein which is incorporated into the viral capsid during retrovirus packaging (4). Plasmid DNA for all three vectors was purified from transformed *E. coli* using Megaprep kits from Qiagen (Valencia, CA). Retroviral vectors (pTJ66, pTJ66-Runx2, and MLV-Gag-RFP) were packaged by transient transfection of helper-virus free ΦNX amphotropic producer cells with plasmid DNA as described elsewhere (1–3, 5).

Scaffold Coating and Cell Seeding. A 0.01% poly(L-lysine) (PLL) solution (70,000–150,000 MW) was used for all studies, as this concentration and charge/molecule ratio yields high levels of virus particle adsorption and transduction efficiency (6, 7). For uniform PLL coating, rectangular collagen scaffolds (3 mm wide × 8 mm long × 2 mm thick, average pore size 61.7 μm, 93.7% pore volume, Kensey Nash, Exton, PA) were immersed in PLL solution for 30 min followed by incubation in Runx2 or empty vector retroviral supernatant for 4.5 h in a humidified 5% CO_2 atmosphere at 32°C. Virus-only control scaffolds were uniformly coated with water followed by incubation in Runx2 retrovirus (R2RV), whereas PLL-only control scaffolds were uniformly coated with PLL followed by incubation in PBS supplemented with 10% FBS. All constructs were washed in Dulbecco's PBS and seeded at a density of 2×10^5 cells per scaffold in osteogenic growth media.

For gradient constructs, the proximal end of collagen scaffolds (5 mm wide × 20 mm long × 2 mm thick) was partially coated by wicking a controlled volume of 0.01% PLL before incubation in Runx2 or empty vector retroviral supernatant for 4.5 h. PLL gradients with differential slopes were generated by dipping collagen scaffolds into a solution of FITC-labeled PLL (100 μg/ml) at a controlled rate using a motorized dip coater (60–700 μm/s dipping speed range). Constructs containing a FITC-PLL gradient were also incubated in RFP-labeled retrovirus (RFP-RV) to visualize retrovirus density within 3-D matrices. These gradient constructs were washed in PBS and seeded at a density of 1×10^6 cells/scaffold in osteogenic growth media.

Cell-seeded constructs were cultured *in vitro* in osteogenic differentiation media (DMEM, 10% fetal bovine serum, 100 units/ml penicillin G sodium, 100 μg/ml streptomycin sulfate, 50 μg/ml L-ascorbic acid, 2.1 mM sodium β-glycerophosphate, 10 nM dexamethasone) until end-point assay.

Cell Viability. Scaffolds were harvested at 42 days postseeding, rinsed in complete Dulbecco's PBS (PBS), and incubated in 4 μM calcein-AM and 4 μM ethidium homodimer-1 (Molecular Probes) in PBS for 30 min under gentle agitation. Constructs were then rinsed (3 × 10 min) in PBS and analyzed with a Zeiss LSM 510 Confocal Microscope using Ar and HeNe lasers and a ×5 objective lens.

DNA Content. Samples were harvested at 1, 21, and 42 days postseeding, rinsed with PBS, and frozen at -80°C. Scaffolds and serially diluted cell standards were thawed, lyophilized, and digested at 55°C in 500 μl of 0.25 mg/ml proteinase K (Fisher Scientific) in 100 mM ammonium acetate (pH 7.0) for 24 h. Digested samples were assessed for DNA content via the PicoGreen dsDNA Quantitation Kit (Molecular Probes). Raw DNA data were converted to cell numbers using a linear standard curve.

Quantitative RT-PCR. Total RNA was isolated at 7 days postseeding using the RNeasy RNA isolation kit with RNAlater stabilization reagent (Qiagen). cDNA synthesis was performed on DNaseI-treated (27 Kunitz units/sample) total RNA (0.25 μg) by oligo(dT) priming using the SuperScript First Strand Synthesis System for RT-PCR (Invitrogen, Carlsbad, CA). Gene expression was assessed by quantitative RT-PCR using SYBR Green intercalating dye (Molecular Probes) and rat-specific primers as previously described (1, 3). Primer specificity was confirmed by ABI Prism 7700 Dissociation Curve Software. Standards for each gene were amplified from cDNA using real-time oligonucleotides, purified using a Qiagen PCR Purification kit, and diluted over a functional range of concentrations. Transcript concentration in template cDNA solutions was quantified from a linear standard curve, normalized to 0.25 μg of total RNA, and expressed as nanomoles of transcripts per μg of total RNA. Detection limits for each gene were determined by reactions without cDNA and fall below the *y*-axis minimum.

Microcomputed Tomography. High resolution x-ray microcomputed tomography (microCT) with a Scanco μCT Medical CT 40 imaging system was used to quantify *in vitro* and *in vivo* mineralization of 3-D scaffolds. Formalin-fixed specimens were scanned at a 16 μm voxel resolution. Uniformly coated scaffolds cultured *in vitro* were evaluated at a threshold corresponding to a linear attenuation of 1.04 cm^{-1}, G filter sigma of 1.2, and filter support of 2. The inner volume of partially coated scaffolds cultured *in vitro* was manually segmented to eliminate edge effects and evaluated between lower and upper thresholds corresponding to linear attenuations of 2.08 cm^{-1} and 3.2 cm^{-1}, respectively. Partially coated scaffolds implanted *in vivo* were evaluated at a threshold corresponding to a linear attenuation of 1.20 cm^{-1}. Reconstructed and thresholded images were evaluated using direct distance transformation methods to calculate mineralized matrix volume within each construct.

Mechanical Testing. For mechanical testing, fresh specimens were washed in PBS, cut in half (gauge length and width of 10-mm and 5-mm, respectively), placed into soft-tissue clamps of an ELF 3200 mechanical testing system (EnduraTEC / Bose), and pulled to failure at a rate of 0.2 mm/sec. Force was recorded using a 11-lb load cell (Interface, Scotsdale, AZ), and displacement recorded via a computer acquisition interface (WinTest, EnduraTEC). Stress and strain were calculated from the force

and displacement data by adjusting for the tissue's cross-sectional area and gauge length, respectively.

Statistical analysis (shown in Fig. 4*C*) indicated that both structural and material mechanical properties were significantly enhanced on the proximal, PLL-coated portion (side A) of R2RV-coated scaffolds compared to control specimens [Mean ± SEM, $n \geq 10$; Max Force at Failure: ANOVA: $P = 0.00012$; *** vs. EVRV side B ($P = 0.000079$), EVRV side A ($P = 0.0437$), and R2RV side B ($P = 0.0089$). Stiffness: ANOVA: $P = 0.0004$; *** vs. EVRV side B ($P = 0.00034$), EVRV side A ($P = 0.035$), and R2RV side B ($P = 0.0122$). Young's Modulus: ANOVA: $P = 0.000067$; ** vs. EVRV side B ($P = 0.000047$) and R2RV side B ($P = 0.005$). Maximum stress: ANOVA: $P = 0.000069$; *** vs. EVRV side B ($P = 0.000044$), EVRV side A ($P = 0.049$), and R2RV side B ($P = 0.0065$)].

s.c. Implantation. Heterogeneous constructs were s.c. implanted into the backs of 7-week-old syngeneic rats after 24 h culture in osteogenic growth media ($n = 3$ for each treatment group). Two implants were placed in each animal, one on each side of a midline incision into s.c. pockets made by blunt dissection. Constructs were explanted after 2 weeks of implantation following euthanasia by CO_2 inhalation. All procedures were carried out according to an IACUC-approved protocol as previously described (5, 8).

Histology and Immunohistochemistry. Formalin-fixed constructs were paraffin embedded and sectioned at 5 μm thickness. Sections were stained with hematoxylin-eosin and von Kossa to observe cellular distribution and matrix mineralization within 3-D constructs, respectively. eGFP expression was observed by immunostaining using a colorimetric avidin-biotin kit (Vector Labs). Sections were deparaffinized, rehydrated, and then pretreated using protease-induced antigen retrieval in 1 μg/ml proteinase K. After pretreatment, slides were incubated in a rabbit polyclonal primary antibody against eGFP (Molecular Probes) followed by sequential incubation in biotinylated anti-rabbit secondary antibody and avidin-biotin linked alkaline phosphatase. Slides were then incubated in Vector Red substrate and counterstained with hematoxylin.

Data Analysis. Unless otherwise stated, all *in vitro* experiments were performed two times in triplicate, each with unique Runx2 retroviral supernatant preparations, and two independent isolates of primary dermal fibroblasts. Data are reported as mean ± standard error of the mean (SEM), and statistical comparisons using SYSTAT 8.0 were based on an analysis of variance (ANOVA) and Tukey's test for pairwise comparisons, with a p value of <0.05 considered significant. To make the variance independent of the mean, statistical analysis of real-time PCR data were performed following logarithmic transformation of the raw data.

1. Phillips JE, Gersbach CA, Wojtowicz AM, Garcia AJ (2006) Glucocorticoid-induced osteogenesis is negatively regulated by Runx2/Cbfa1 serine phosphorylation. *J Cell Sci* 119:581–591.
2. Byers BA, Pavlath GK, Murphy TJ, Karsenty G, Garcia AJ (2002) Cell-type dependent up-regulation of in vitro mineralization after overexpression of the osteoblast-specific transcription factor Runx2/Cbfal. *J Bone Miner Res* 17:1931–1944.
3. Gersbach CA, Byers BA, Pavlath GK, Garcia AJ (2004) Runx2/Cbfa1 stimulates transdifferentiation of primary skeletal myoblasts into a mineralizing osteoblastic phenotype. *Exp Cell Res* 300:406–417.
4. Sherer NM, *et al*. (2003) Visualization of retroviral replication in living cells reveals budding into multivesicular bodies. *Traffic* 4:785–801.
5. Phillips JE, Hutmacher DW, Guldberg RE, Garcia AJ (2006) Mineralization capacity of Runx2/Cbfa1-genetically engineered fibroblasts is scaffold dependent. *Biomaterials* 27:5535–5545.
6. Davis HE, Rosinski M, Morgan JR, Yarmush ML (2004) Charged polymers modulate retrovirus transduction via membrane charge neutralization and virus aggregation. *Biophys J* 86:1234–1242.
7. Gersbach CA, Coyer SR, Le Doux JM, Garcia AJ (2007) Biomaterial-mediated retroviral gene transfer using self-assembled monolayers. *Biomaterials* 28:5121–5127.
8. Phillips JE, Guldberg RE, Garcia AJ (2007) Dermal fibroblasts genetically modified to express Runx2/Cbfa1 as a mineralizing cell source for bone tissue engineering. *Tissue Eng* 13:2029–2040.

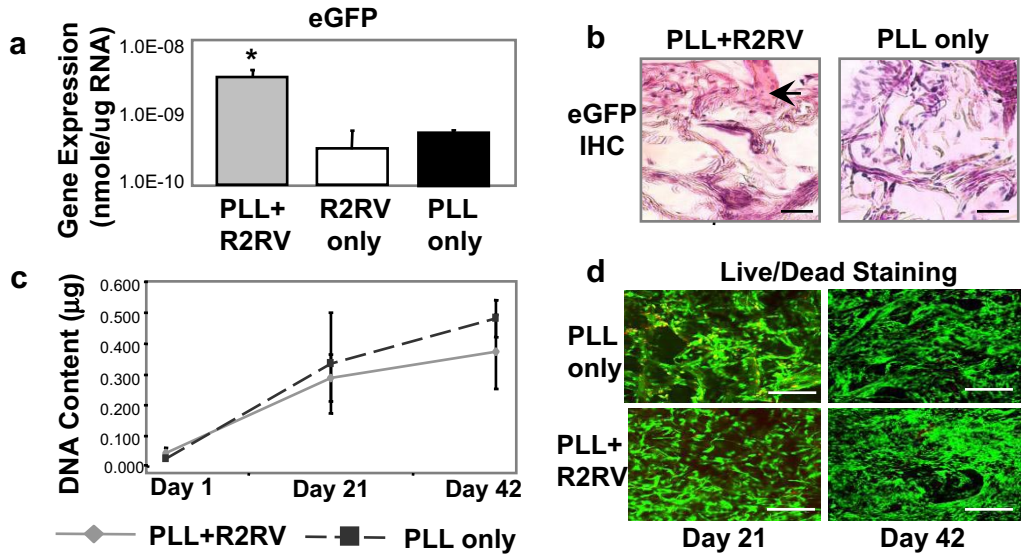

Fig. S1. Biomaterial-mediated retroviral gene transfer is a feasible strategy for genetic modification of fibroblasts. Scaffolds were uniformly coated with the cationic polypeptide PLL before incubation in negatively-charged Runx2 retrovirus (R2RV). Primary dermal fibroblasts were then seeded onto these scaffolds and cultured *in vitro* until endpoint assay. (*a*) eGFP mRNA levels were up-regulated in PLL+R2RV-coated scaffolds compared to controls at 7 days postseeding, demonstrating that fibroblast transduction is dependent on precoating scaffolds with PLL [Mean + SEM, $n = 3$; ANOVA: $P = 0.05$; * different from R2RV only control ($P = 0.0499$)]. (*b*) The spatial localization of transduced cells within collagen scaffolds was confirmed by immunohistochemical staining of histological sections for eGFP expression (pink, arrow) and hematoxylin counterstain (blue). (Scale bar: 50 μm.) (*c* and *d*) Uniform cellular colonization and viability at the periphery of collagen scaffolds throughout the 42 day culture period was confirmed by (*c*) quantification of DNA content (Mean + SEM, $n = 3$; ANOVA: $P = 0.032$) and (*d*) confocal microscopy image analysis of live (green)/dead (red) fluorescence staining. (Scale bar: 500 μm.)

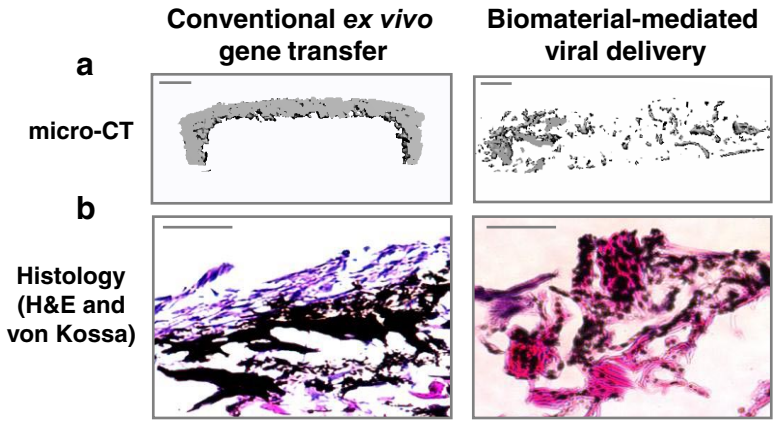

Fig. S2. Fibroblast colonization and mineral deposition patterns are differentially modulated by virus delivery strategy. (*a*) Cross-sectional microCT images depicting the distribution of mineralized matrix within Runx2-engineered constructs. (Scale bar: 1 mm.) (*b*) Cell and mineral distribution within collagen disks was visualized by hematoxylin-eosin (H&E, blue&pink) and von Kossa (black) staining, respectively. (Scale bar: 250 μm.) Mineral deposits displayed a dense morphology and were confined to the periphery of scaffolds seeded with fibroblasts engineered by conventional ex vivo gene transfer techniques. In contrast, discrete mineralized nodules were distributed throughout the interior of scaffolds coated with Runx2 retrovirus prior to fibroblast seeding.

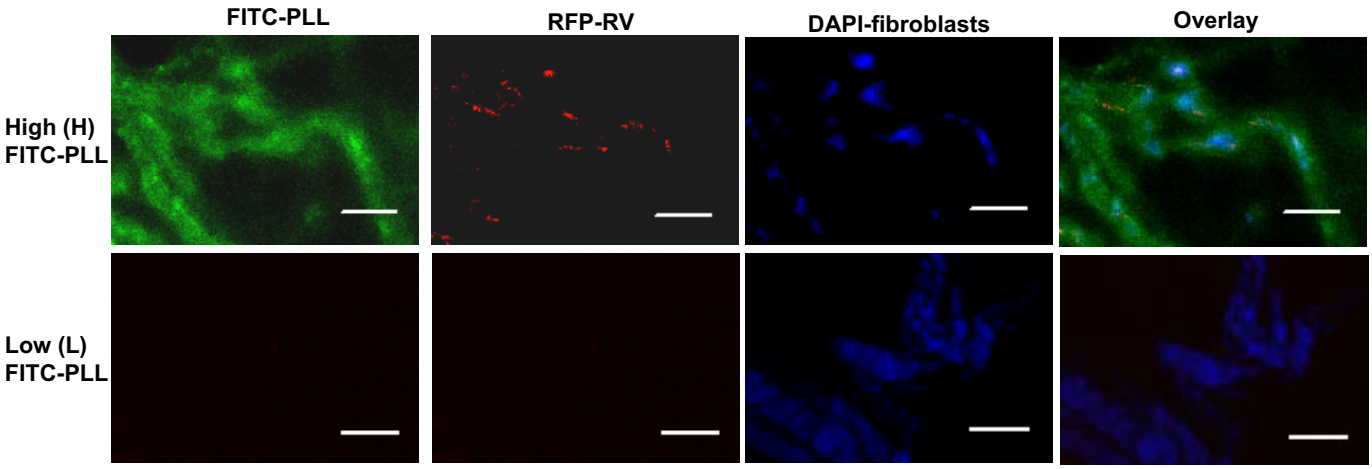

Fig. S3. Spatial distribution of PLL-mediated retrovirus immobilization. Collagen scaffolds were partially coated with FITC-labeled PLL (FITC-PLL) at a dipping speed of 170 μm/s and incubated in red fluorescent protein-labeled retrovirus (RFP-RV) before cell seeding. High magnification confocal microscopy images at high (H) and low (L) FITC-PLL densities (green) at 12 h postseeding revealed that RFP-RV (red) co-localized with DAPI-stained fibroblast nuclei (blue) in construct region containing the highest PLL intensity. RFP-RV intensity decreased gradually moving lengthwise down the *z* axis toward the distal end, while DAPI-stained nuclei show equivalent cell densities throughout the construct *z*-axis cross-section. (Scale bars: 10 μm.)